Field Evaluation of a Low-Cost Strapdown IMU by means GPS

RAUL DOROBANTU[*)] AND BENEDIKT ZEBHAUSER[*)]

Abstract

The paper presents a field experiment for a low-cost strapdown-*IMU/GPS* combination, with data postprocessing for the determination of 2-D components of position (trajectory), velocity and heading. In the present approach we have neglected earth rotation and gravity variations, because of the poor gyroscope sensitivities of our low-cost *ISA* (Inertial Sensor Assembly) and because of the relatively small area of the trajectory. The scope of this experiment was to test the feasibility of an integrated *GPS/IMU* system of this type and to develop a field evaluation procedure for such a combination. Also a hardware synchronisation between *GPS* time and the *IMU*'s data acquisition time scale is presented.
The authors briefly describe the *IMU* strapdown mechanisation procedure, the *DGPS* data processings and the implementation of a suboptimal Linear Kalman Filter (*LKF*), with the system linearization exemplified for the 2-D case.
Plots of test results, concerning the *KF* update for the carrier phase or pseudorange *DGPS* solutions, made at regular epochs of integer seconds, as well as comparisons between the *INS* and the *GPS* trajectory solutions are given. The results demonstrate the feasibility of our cost-effective *IMU/GPS* integration, with accuracy improvements from ca. 20 m (*IMU* alone) toward the meter domain (for the combination) depending on good *GPS* reception conditions. The precise carrier-phase *DGPS* solution, with an accuracy in the *cm* domain, was used as reference for the strapdown-mechanized-*IMU*'s performance evaluation.

I. Introduction

Since 1978 one has recognised the advantages of tightly-coupled *GPS/INS* (Global Positioning System /Inertial Navigation System) systems [1]. The idea is to combine the advantage of the short-term precision of *INS* and the long-term stability of *GPS*. With the significant decrease of inertial sensor prices [2, 3] (micromachined accelerometers and rate gyroscopes), the rapid increase of computing power (permitting the on-line approach applied to strapdown navigation systems) and with the tendency of using standard software for such *GPS/INS* systems [1], one can look forward for a much wider use of aided *GPS* inertial navigation. The goal of this paper is to present the results from a field test with a combination of a low-cost strapdown *ISA* (Inertial Sensor Assembly) unit [4] with *GPS* aiding. A central item has been the test of the feasibility of a processing algorithm

Fig. 1: *The rover car and the stationary receiver on the start point*

[*)] Technische Universität München, Institut für Astronomische und Physikalische Geodäsie
Arcisstr. 21, D-80290 München, Germany; **email: raul@alpha.fesg.tu-muenchen.de**

using a simplified linear Kalman filter [5, 6] with only 5 state-variables. A 2-D solution of this type benefits from the precision information of position, velocity and heading, derived from a reference *carrier-phase DGPS* (Differential *GPS*) solution; a variety of simulations runs has been carried out with two specific *GPS* solutions (Pseudorange and carrier phase *DGPS*).
The study has also permitted to elaborate a field test methodology for *IMU* (Inertial Measurement Unit) units. The tests have carried out with a car carrying on its roof a platform equipped with two *GPS*-antennas and one *IMU* unit. There are neglected the **g** - variations and the Earth rotation rate, because of the small dimensions of the test area (some 100×100 m), of the relative low car velocities (about 5 m/s, that is about 18 km/h) and of the reduced rate sensitivity of the used gyroscopes.
The mutual benefit of an *INS/GPS* combination should be the compensation of the *IMU*(*INS*) drift and the coverage of long period unavailability of the *GPS* [7] (in city environments, in tunnels, etc.) or of imprecision caused by interference by multipath reflections. By using an appropriate suboptimal Kalman filter (*KF*), one can take advantage of a good dynamic description of the *IMU*, combined with the unbiased observations of the available *GPS* data.
In the paper the *INS/GPS* measuring system is described. We also give an *IMU* strapdown compensation algorithm (implemented also in an interactive version under *Simulink* - *Matlab*) and the postprocessing solution for a reference navigation path, together with some alternative *KF* simulations (observations provided every second and every 4 s respectively or with random *GPS* updating).

II. Experiment description

In Fig. 1 the rover car is shown equipped with two *GPS* receiver antennas mounted on the car roof on a wooden plate at a fixed distance of 1.40 m. One can see the *ISA* unit, rigidly fixed in the middle of the platform. A stationary *GPS* receiver is used to generate the *DGPS* (Differential *GPS*) solutions.
The *GPS* system permits the accurate computation of the position (carrier-phase *DGPS*) and the velocity of the *ISA*'s centre of mass. One can also derive a heading reference from the *GPS* solution and deliver it as update for the angular azimuth in the *KF* (normally furnished from the *z*-axis rate gyroscope).

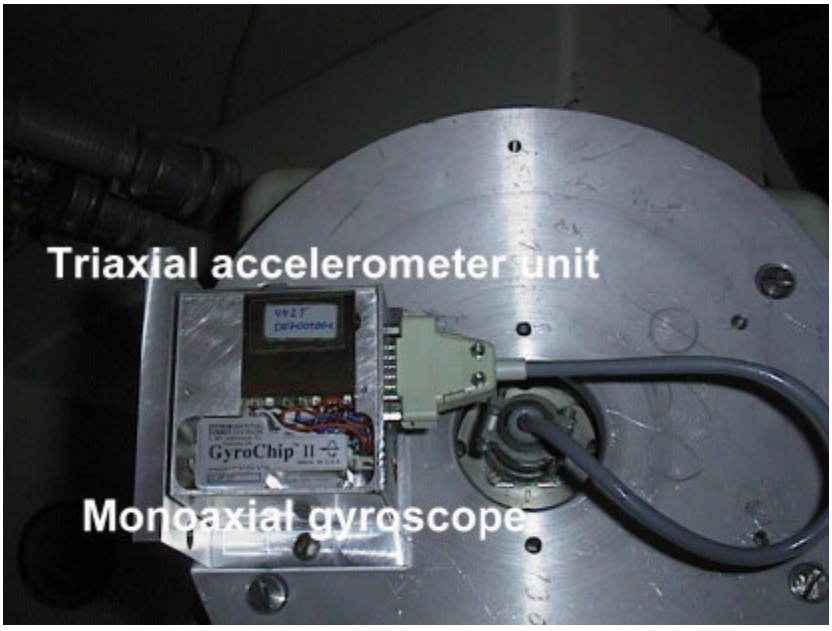

Fig. 2 *View of the opened ISA unit: the three-axial accelerometer and a one-axis gyroscope*

This first test has been carried out on „Theresienwiese“ in Munich.
The *ISA* unit, of type *iMAR* ® [4], uses a triaxial accelerometer realised by quartz micromachined technology [8] and a triad of quartz vibrating rate gyroscopes [9], based on the Coriolis-force principle.
The inertial sensors are mounted in an aluminium cube by *iMAR* ® with an unique reference mounting surface. Fig. 2 shows the opened cube, here mounted on a rotating platform for calibration in our laboratory.
The analog signal furnished by the *ISA* unit is acquired via an *A/D* multiplexed conversion unit (Type DAQPad - MIO - 16XE - 50 from *NATIONAL INSTRUMENTS* ® [10]), with a 16 bit/channel resolution. A sampling rate of 25 Hz was chosen; data are stored on a *TOSHIBA* ® PC - Notebook in binary or ASCII format files, with 8 columns: 3 channels of accelerometer data, 3 channels of gyroscope data (the rotating rate information), one channel of the inertial-cube interior temperature information and one channel with time-reference information (in analog form), necessary to assure the synchronisation between the *INS* and the *GPS* systems.
In this starting phase of the experiment the synchronisation is carried out by simultaneous continuous registration, on the 8-th channel (#7) of the data converter, of a time signal with 0.1 s duration. It is derived from the standard *PPS* (one Pulse Per Second) output signal of a *GPS* receiver (here, for comparison, derived from an *ASHTECH* ® receiver, respectively from the rover *TRIMBLE* ® receiver). To realise also an absolute reference time scale, a supplementary 0.5 s asynchronous signal is generated manually, at an arbitrarily observed *GMT* time, displayed on the *GPS* receiver panel, and electronically superimposed to the same # 7 channel of the time reference (see Fig. 3).
The realised electronic (the monostable multivibrators, the logic *OR* and the attached *LED* displays - for the *PPS* signal, respectively for the asynchronous one) is mounted in a small separate case (see Fig. 4) and connected by coaxial cables to the *PPS* output signal (*GPS* receiver) and the input of the 8-th channel of the *A/D* converter.
Because of the great duration difference (5:1) between the two time signals one can automatically detect any asynchronous event without difficulty. This enables an absolute marking of the inertial data registration on the associated time scale.

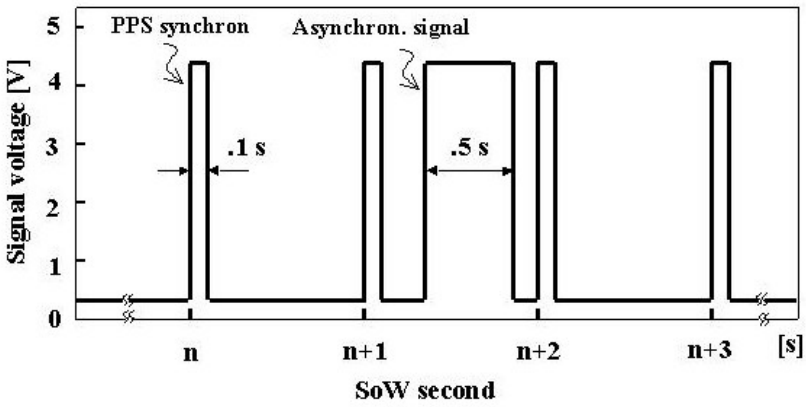

Fig. 3 *Time scale generated on the 8-th channel of the inertial data file (PPS synchronous and asynchronous event signals)*

Nevertheless one must take into account the absolute time difference between the recorded *UTC* asynchronous event and the *GPS*-time reference *SoW* (Second of *GPS* Week) for the satellite positioning solution. At the time of the experiment this difference was [11]:

GPS-time - *GMT-time* = +12 s (i.e., at 14.05.1998 the *GPS* time was 12 s ahead of *UTC*) .

In this 2-D experiment no initial alignment was carried out. The alignment is deduced in the course of the experiment from the *GPS* positioning data. Of course, one must take into account a short initialisation phase of about 10 to 15 min at the beginning of the *GPS* session.

Fig. 4 *View of the hardware for the analog time signals (in the laboratory experimentation phase, connected to a Trimble GPS receiver)*

III. IMU's strapdown mechanisation

Using the calibration data for the inertial sensor assembly (bias, linear scale factors, gyroscopes triad non-orthogonality) delivered from the manufacturer and the supplementary calibration measurements made in our laboratory the error model of the inertial sensors is validated. The most important measurements carried out in our laboratory are: the evaluation of the noise behaviour of the inertial data sets, static accelerometer calibrations - to determine the supplementary non-linear terms of the static transfer characteristics, considered only to degree 2 -, as well as the establishment of the non-linear time and temperature behaviour of the accelerometer's drift and scale factors and the non-orthogonality of the accelerometer's triad. The complex dependencies between the electrical output signal u [V] of an inertial sensor (here an accelerometer) and the specific forces f, the elapsed time t and the temperature T take the following analytical form:

$$u = D + H + k_0 + k_{01}\cdot t + k_{02}\cdot t^2 + k_1\cdot f_1 + k_2\cdot f_1^2 + k_3\cdot f_1^3 + k_{12}^{no}\cdot f_2 + k_{13}^{no}\cdot f_3 + \\ + k_{12}^{cc}\cdot f_1\cdot f_2 + k_{13}^{cc}\cdot f_1\cdot f_3 + k_{41}\cdot T + k_{42}\cdot T^2, \qquad (1)$$

where we used the following notation:

D = dead zone (under this threshold one has no signal),
H = hysteresis,
k_0 = bias (a new value for each new use of the instrument),
k_{01}, k_{02} = drift coefficients (modelling the linear and the quadratic variations with time t, respectively),
k_1, k_2, k_3 = coefficients of the polynomial approximation of the non-linear response characteristic to the specific force along the sensible input axis,
f_1, f_2, f_3 = specific forces, along the three input axes (denoted 1, 2 and 3),
k_{12}^{no}, k_{13}^{no} = coupling coefficients between the input axes, due to *n*on-orthogonality,
k_{12}^{cc}, k_{13}^{cc} = cross - coupling coefficients,
k_{41}, k_{42} = coefficients of the polynomial dependence (linear and quadratic) of the sensor output signal from temperature T

The inertial data are processed in a strapdown mechanisation [12], based on the following expression for a one-component specific force in a body reference system (see Fig. 5, that explains the forces

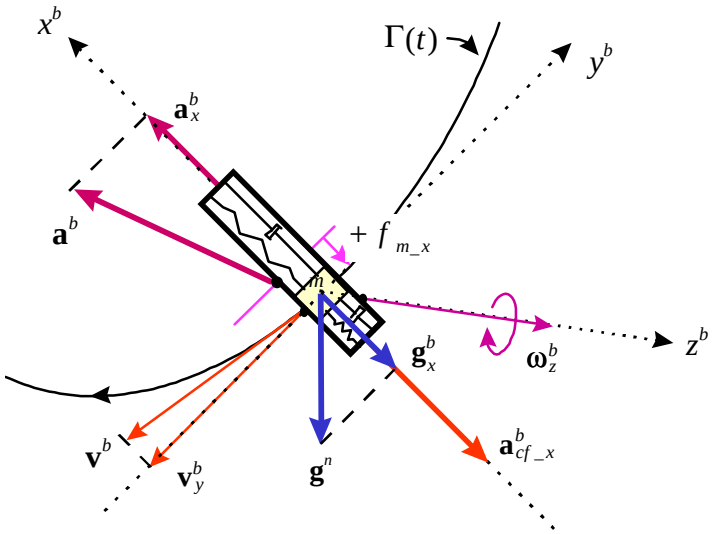

Fig. 5 *Specific force as a function of the acceleration components along a reference system firmly attached to the moving body (example for x - axis)*

considered, acting upon the seismic mass of the accelerometer), as a function of the linear acceleration a_x^b, the apparent centripetal acceleration $a_{cf\_x}^b$ and the corresponding axial component of the static gravitational acceleration g_x^b (the superscripts b denote the vector components in the *body* reference system):

$$f_{m\_x} = a_x^b + a_{cf\_x}^b - g_x^b . \qquad (2)$$

The corresponding vectorial form (with the specific force vector now denoted by **a** and the correction terms of centripetal and gravity acceleration expressed in the body coordinate system) is:

$$\mathbf{a}^b = \mathbf{a} - \boldsymbol{\omega} \times \mathbf{v}^b + \mathbf{C}_n^b \cdot \mathbf{g}^n . \qquad (3)$$

with:

$\boldsymbol{\omega}$ = the angular velocity vector,

$\mathbf{v}^b$ = the velocity vector, given in the coordinate system b,

$\mathbf{C}_n^b$ = the rotation matrix from the local coordinate system n to the body coordinate system b.

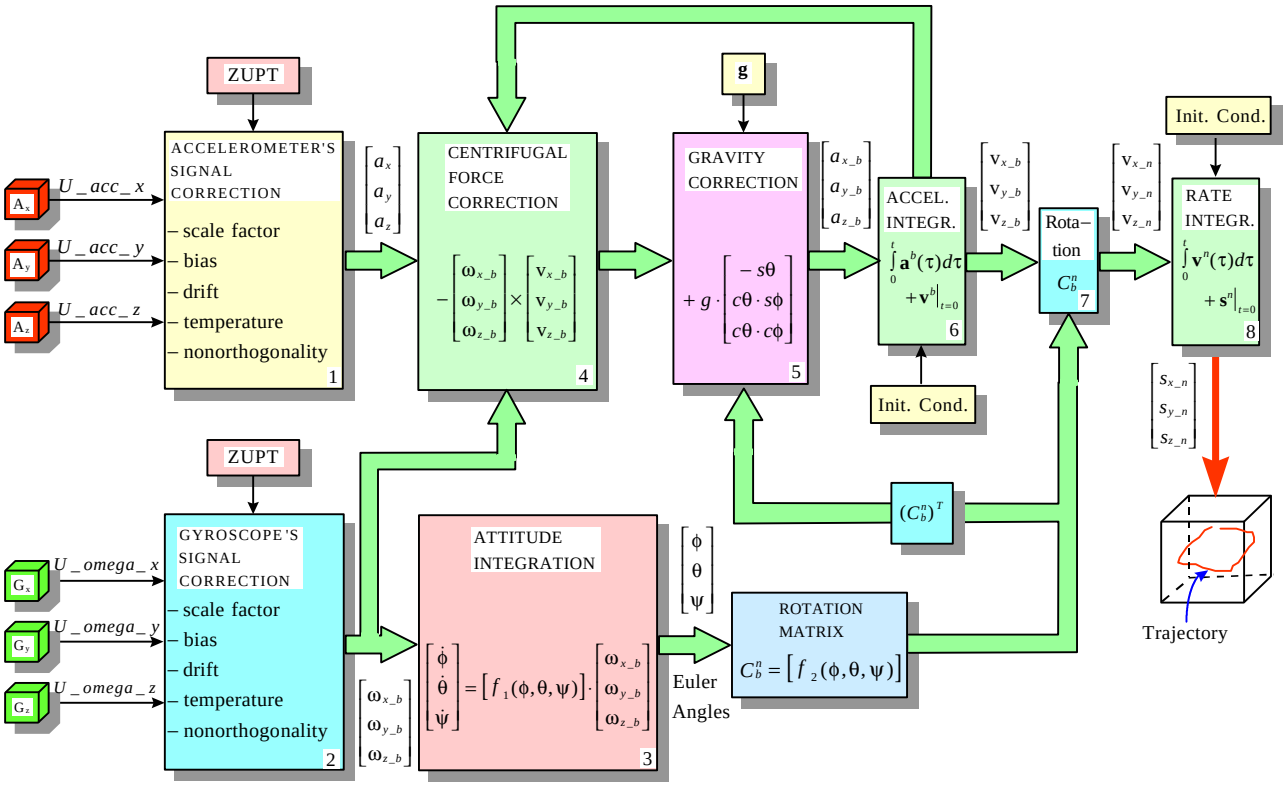

Fig. 6 *Flow-chart of the strapdown mechanisation*

In this approach we only take into account the apparent centrifugal forces and the tilt-induced static accelerations (components of **g** assum ed to be constant). Neglected is the small Coriolis force acting on the moving mass as a consequence of the rotation of the inertial sensors case.

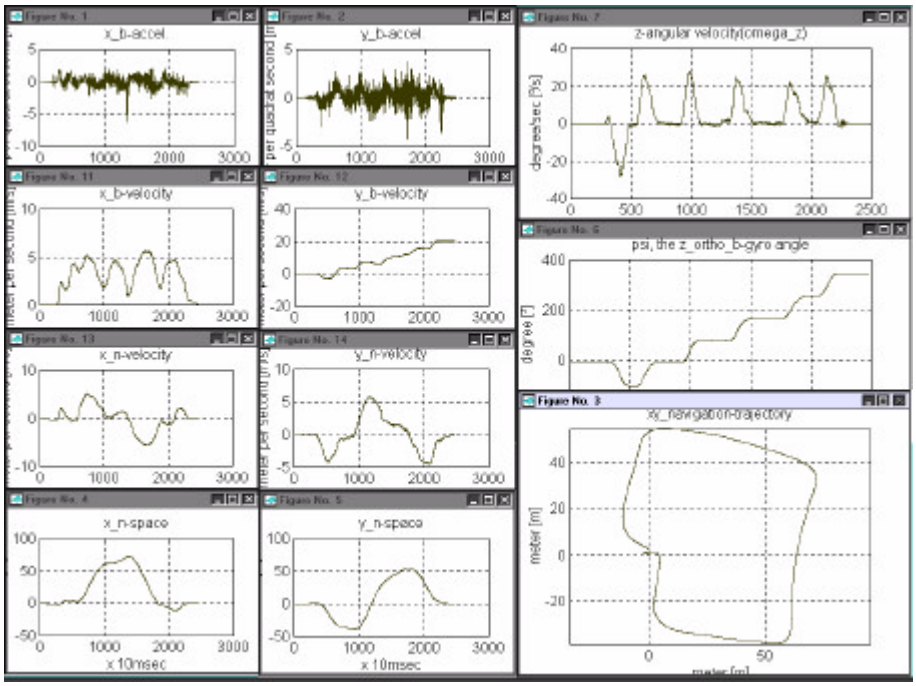

Fig. 7 S*trapdown mechanisation solution of the IMU*

a | e | i
b | f | j
c | g | k
d | h | k

a - *x-axis body acceleration*
b - *x-axis body velocity*
c - *x-axis velocity in the pseudo-inertial reference system*
d - *x-axis position in the pseudo-inertial reference system*
e - *y-axis body acceleration*
f - *y-axis body velocity*
g - *y-axis velocity in the pseudo-inertial reference system*
h - *y-axis position in the pseudo-inertial reference system*
i - *rotation rate about the z-axis*
j - *rotation angle* ψ *about the z-axis*
k - *x/y trajectory (only from inertial data)*

As mentioned above we neglect the **g** - variations because of the relative small experimental area and also the Coriolis force component resulting from the earth rotation (both of them because of lack of sensitivity of the low-cost inertial sensor system).
The flow-chart of the algorithm is given in the Fig. 6. The program has been written in the *Simulink - Matlab* language, which enables a transparent and interactive design of the whole diversity of signals, also permitting an easy and rapid proof of the error model parameters.
In the Fig. 7 the inertial solution of the *x/y* trajectory, as well as the rotation angle ψ (about the *z*-axis) are presented.

IV. GPS solution

The *GPS* solution was accurately determined by *carrier phase DGPS* data evaluation using *OTF*-(*On-The-Fly*) techniques, processed with the commercial *SPECTRA PRECISION GEOGENIUS* ® software. Two separate solutions were computed, one for each pair of reference/rover receivers.
Each point of the resulting trajectory of the *ISA*'s centre of mass (plotted as reference in the Fig. 14) represents a position solution, spaced regularly at 1 s intervals. Considered was the center point between the two *GPS* antennas, matched with the centre of the inertial cube. The trajectory and the rotation angle are determined consequently (as the arithmetic mean of successive positions of the two rover antennas and as the rotation angle of the spatial vector defined by the two phase centres of the mobile receiver antennas respectively).

Some remarks concerning the GPS solutions performed:

Because a standalone *GPS* receiver position solution only yields an accuracy/repeatability of some tens of meters it is common to perform measurements with 2 receivers (or more) simultaneously.

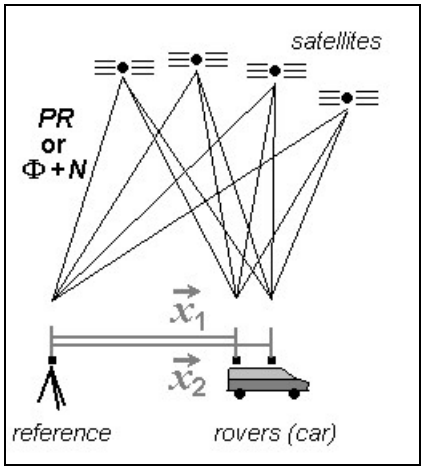

Fig. 8 *DGPS constellation with 2 rover antennas on top of the car, showing the observables as well as the estimated difference vectors between reference and rovers*

Thereby one receiver is held stationary at a reference position *A* nearby the planned trajectory of the second (moving) receiver *B*, the so called rover. This is called *DGPS*. See Fig. 8 for the constellation in this experiment with
$\vec{x}_1 = [\Delta X, \Delta Y, \Delta Z]^T_{antenna\,1}$, $\vec{x}_2 = [\Delta X, \Delta Y, \Delta Z]^T_{antenna\,2}$.

By processing the simultaneous pseudorange measurements *PR* from the two receivers by the double differencing technique, we can eliminate systematic time dependent errors like satellite and receiver clock biases. We can reduce other effects too and avoid, in addition, problems with high correlations in the parameter estimation process.
The double difference observable for *pseudorange DGPS* can be written:

$$\Delta\nabla^{jk}_{AB} = PR^k_B - PR^k_A - \left(PR^j_B - PR^j_A\right) = S^k_B - S^k_A - \left(S^j_B - S^j_A\right) + e \qquad (4)$$

with: *PR* = pseudorange,
S = geometric distance between receiver A,B and satellite j,k ,
e = unmodeled errors (multipath, atmospheric effects) and noise.

The result of a least squares adjustment using these double difference observations provides position differences or strictly speaking vector components ΔX, ΔY, ΔZ in a geocentric Cartesian coordinate system describing the vector between the reference and the rover receiver or rather between their antennas. This technique using pseudoranges yields an accuracy/repeatability of about 1 meter for epochwise solutions in kinematic applications. Smoothing of the pseudoranges *PR* by means of carrier phases can bring down this value to some decimeters.
For even higher accuracy of a few centimeters one has to compute the position differences using carrier phase observations Φ: In contrast to pseudoranges *PR*, that are equivalent to distance measurements between satellite and receiver, carrier phase measurements require the determination of cycle ambiguities *N*, because at the measurement epoch only the received carrier phase (fractional part of a cycle with $\lambda \cong 20$ cm) and the change in the integer part (full cycles) are registered (combined in Φ), while the full range remains unknown.
The double difference observable for *carrier phase DGPS* can be written:

$$\Delta\nabla^{jk}_{AB} = \Phi^k_B - \Phi^k_A - \left(\Phi^j_B - \Phi^j_A\right) = \frac{f}{c_0}\left(S^k_B - S^k_A - \left(S^j_B - S^j_A\right)\right) - N^{jk}_{AB} + \varepsilon \qquad (5)$$

with: $N^{jk}_{AB} = N^k_B - N^k_A - \left(N^j_B - N^j_A\right)$ double difference ambiguity,
Φ = carrier phase observable,
S = geometric distance between receiver A,B and satellite j,k ,
f = carrier frequency,
c_0 = speed of light in vacuum,
e = unmodeled errors (multipath, atmospheric effects) and noise.

For further information on *GPS* techniques see also [13, 14, 15].
Regarding the kinematic application we are again forced to get epochwise position solutions. Thus in contrast to stationary case we cannot accumulate observations to get higher redundancy for the estimation process which would allow us to determine these ambiguity parameters more easily. Instead we have to resolve them "*on-the-way*" (*on-the-fly*). For high precision positions we have to fix the ambiguity parameters (they are integers) in the position estimation process to their true values. Because the true integer values cannot reliably be found by rounding the actual float values from the least squares adjustment, they must be searched by statistical tests like χ^2-tests on the residuals of a position solution after introducing a set of possible double difference integer ambiguities, or like FISHER-tests on the ratio between the best and the second best - from the statistical point of view - position solution from different possible integer ambiguity sets. In the software we used (*SPECTRA PRECISION GEOGENIUS* ®) the search is performed with a polynomial approach (linear regression) of the residuals in order to increase the computational speed. The search hyperspace of all possible ambiguity sets is defined by a 30σ interval for every double difference ambiguity around its float solution. When the "true" set of all (n_{sat}-1) double difference integer ambiguities is found, they are held fixed and the positions per epoch can be solved exactly .
For further information on *DGPS* and ambiguity resolution techniques see also [16, 17].
For comparison purposes the geocentric Cartesian coordinates are transformed into a local projection to yield north, east and up components ΔN, ΔE, ΔU (≡-ΔD) instead of ΔX, ΔY, ΔZ.

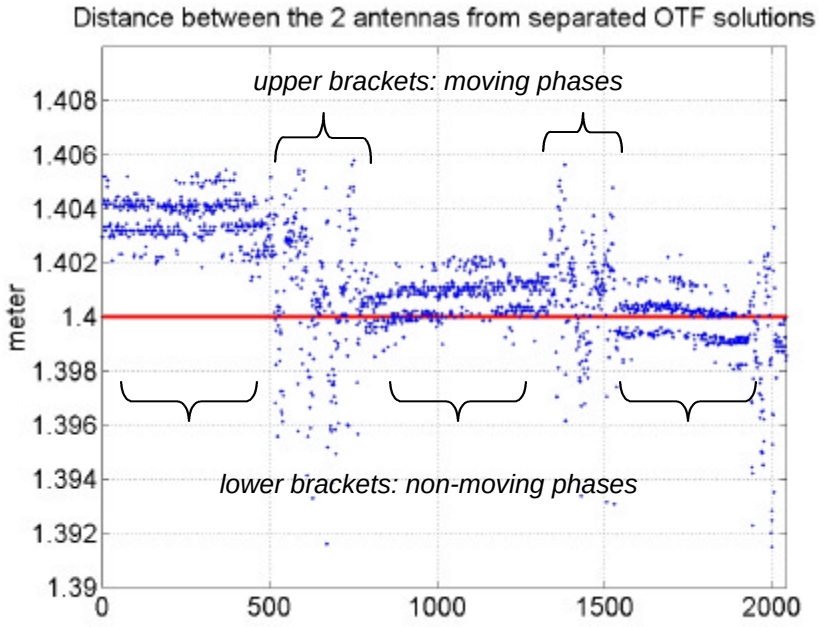

Fig. 9 *GPS solution of the constant distance (1.40 m) between the two rover antennas (the greatest errors are produced during the test rides)*

For a better insight into the accuracy of the *OTF-GPS* solutions we have plotted the time evolution of the constant baseline between the two rover antenna centres, in reality always 1.40 m, determined from two independent *GPS* solutions. From Fig. 9 one can see maximal errors about +/- 5 mm, also during the intervals of car movement. It should be noted that systematic errors affecting both antennas in the same way, that may reach up to 1 cm, are neglected in such an analysis.

The precise carrier phase *DGPS* solution, as well as the pseudorange *DGPS* solution with a precision in the meter domain, can also be used as a bias free observation in the Kalman filter.
One can derive from the *GPS* solution the approximate *x*-axis velocities, expressed in [m/s] as:

$$v_X = (x_{t_k} - x_{t_{k-1}}) / \Delta t \,, \qquad (6)$$

by considering the equal time-interval Δt of the *GPS* solutions and determined each second (similarly for the *y* component), or, more elegantly, by computing the time derivatives of the smoothly interpolated trajectory.

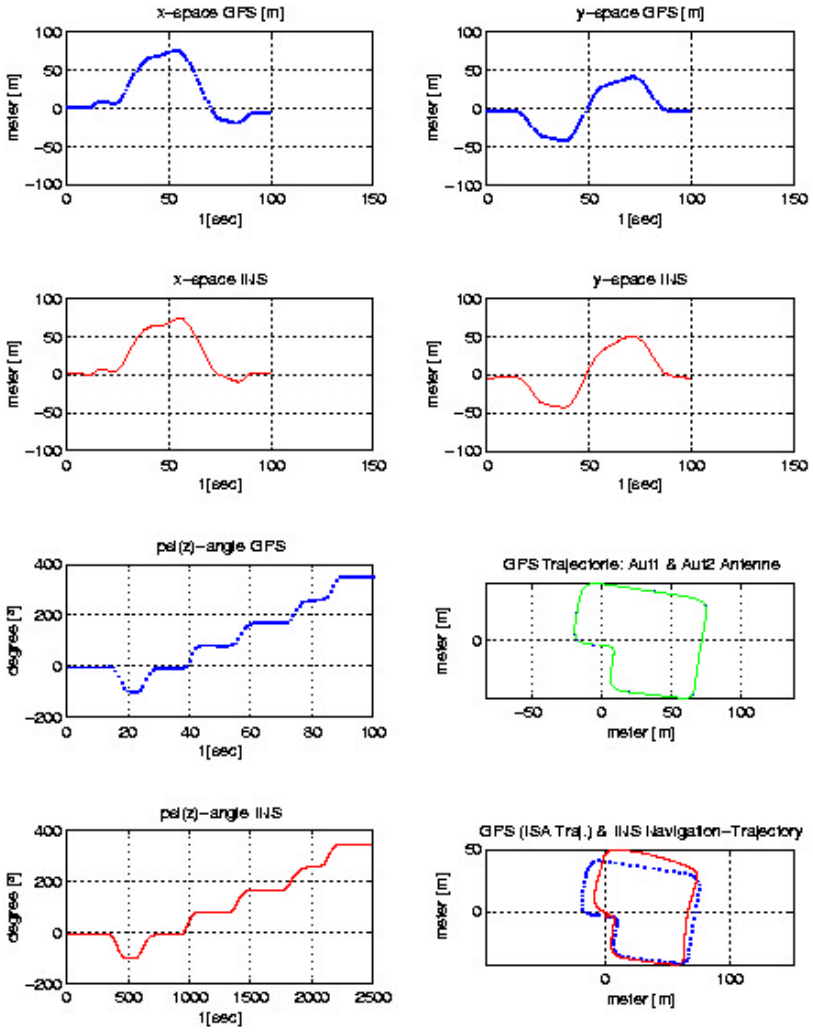

Fig. 10 *Comparison between the GPS and INS solutions (both of them given in a pseudo-inertial reference system)*

a	e
b	f
c	g
d	h

a - *x-axis space: GPS solution*
b - *x-axis space: INS solution*
c - *rotation angle* ψ *: GPS solution*
d - *rotation angle* ψ *: INS solution*
e - *y-axis space: GPS solution*
f - *y-axis space: INS solution*
g - *x/y trajectory*: *GPS solution*
h – independent *INS and GPS trajectories*

From the comparison between the *GPS* and *INS* solutions, presented in Fig. 10, one can see the good match of the *x/y* trajectories and the azimuth solutions (a detailed comparison evidenced differences of under one degree, after an appropriate correct alignment). One can see also the permanently decreasing match of the *IMU* - determined trajectory, because of the continuously increasing unmodeled drift error components with time.

V. Integrated *INS/GPS* solution of the trajectory

To check the feasibility and the usefulness of the integration of our low-cost *IMU* with *GPS*, we built several different Kalman filter configurations, all working in the 2-D (two-dimensional) domain, taking into account the accurate carrier phase *DGPS* solution with an update every second - as well as with some slower or a random epoch updating (every 4 s or randomly ($\sigma = 4$ s)). A further test was the use of the pseudorange *DGPS* solution. The *INS(IMU)* strapdown trajectory solution, with short term precision, but long term drifts, is corrected either on-line or post-mission by means of the bias-free observations furnished by the *GPS* aiding. We made also tests for aiding every second.

We used a *LKF* (Linear Kalman Filter), with the *IMU* trajectory as reference. Because of the short duration of our experiment, there are no noticeable temperature variations in the inertial sensor unit; so we applied in this test only a coarse bias correction at the beginning, neglecting scale-factor variations; the compensated inertial sensor drifts are modelled only as linear time variations. Of course, the complete algorithm must consider both the non-linear shape of the transfer characteristics of gyroscopes and accelerometers, as well as the polynomial time and temperature dependencies of the drifts. It models the slow variable drifts as Gauss-Markov processes.

The local reference system *NED* (North, East, Down) (denoted here with *n*), in which the reference trajectory of the *LKF* is established (as solution of the *IMU* with the strapdown mechanisation), can be assumed for this test to be an inertial frame. The linearized solution is obtained by Taylor expansion of the real non-linear trajectory model about the reference trajectory, retaining only the first order term [5, 6].
From the non-linear plant and observation models, in the continuous-time domain:

$$\dot{\mathbf{x}} = \mathbf{f}(\mathbf{x}, \mathbf{u}_d, t) + \mathbf{G} \cdot \tilde{\mathbf{u}}(t)$$
$$\mathbf{z} = \mathbf{h}(\mathbf{x}, t) + \tilde{\nu}(t), \tag{7}$$

where $\tilde{\mathbf{u}}(t)$, $\tilde{\nu}(t)$ are the Gaussian white noise processes of the dynamic system, respectively of the observation, we deduce [6]:

- the discrete time non-linear model:

$$\mathbf{x}_k = \mathbf{f}(\mathbf{x}_{k-1}) + \tilde{\mathbf{w}}_{k-1}$$
$$\mathbf{z}_k = \mathbf{h}(\mathbf{x}_k) + \tilde{\nu}_k \tag{8}$$

(with $\tilde{\mathbf{w}}_k \sim N(0, \mathbf{Q}_k)$, $\tilde{\nu}_k \sim N(0, \mathbf{R}_k)$),

- the reference trajectory model (without noise):

$$\mathbf{x}_k^* = \mathbf{f}(\mathbf{x}_{k-1}^*, \mathbf{u}_d), \tag{9}$$

- the linearized perturbed trajectory model:

$$\delta \mathbf{x}_k = \left.\frac{\partial \mathbf{f}(\mathbf{x}, \mathbf{u}_d, k)}{\partial \mathbf{x}}\right|_{\mathbf{x}=\mathbf{x}_{k-1}^*} \cdot \delta \mathbf{x}_{k-1} + \tilde{\mathbf{w}}_k \tag{10}$$

(with the definition of the perturbation from the nominal: $\delta \mathbf{x}_k \triangleq \mathbf{x}_k - \mathbf{x}_k^*$),

and the linearized observation model:

$$\delta \mathbf{z}_k = \left.\frac{\partial \mathbf{h}(\mathbf{x}, k)}{\partial \mathbf{x}}\right|_{\mathbf{x}=\mathbf{x}_{k-1}^*} \cdot \delta \mathbf{x}_{k-1} + \tilde{\nu}_k . \tag{11}$$

For the derivation of the explicit forms of the above defined Jacobian matrices (the discrete linearized state transition matrix: $\Phi_{k-1} = \left.\frac{\partial \mathbf{f}(\mathbf{x}, k)}{\partial \mathbf{x}}\right|_{\mathbf{x}=\mathbf{x}_{k-1}^*}$ and the linear observation matrix $\mathbf{H}_k = \left.\frac{\partial \mathbf{h}(\mathbf{x}, k)}{\partial \mathbf{x}}\right|_{\mathbf{x}=\mathbf{x}_k^*}$), we are first considering the general three-dimensional form of a continuous state equation system for a strapdown mechanisation of a body (materialised as a triad, also with all lever-arm effects omitted), moving in the reference system *n* assumed to be inertial:

$$\begin{bmatrix} \dot{\mathbf{s}}^n \\ \dot{\mathbf{v}}^n \\ \dot{\Psi}^n \end{bmatrix} = \begin{bmatrix} \mathbf{0} & \mathbf{I} & \mathbf{0} \\ \mathbf{0} & \mathbf{0} & \mathbf{0} \\ \mathbf{0} & \mathbf{0} & \mathbf{0} \end{bmatrix} \cdot \begin{bmatrix} \mathbf{s}^n \\ \mathbf{v}^n \\ \Psi^n \end{bmatrix} + \begin{bmatrix} \mathbf{I} & \mathbf{0} & \mathbf{0} \\ \mathbf{0} & \mathbf{C}_b^n(\Psi) & \mathbf{0} \\ \mathbf{0} & \mathbf{0} & \mathbf{E}(\Psi) \end{bmatrix} \cdot \begin{bmatrix} \mathbf{0} \\ \mathbf{a}^b \\ \boldsymbol{\omega}^b \end{bmatrix} + \mathbf{G} \cdot \tilde{\mathbf{u}}(t) \tag{12}$$

where we denote:

$\mathbf{s}^n = [s_{x\_n} \;\; s_{y\_n} \;\; s_{z\_n}]^T$, the position vector in the coordinate system *n*

$\mathbf{v}^n = [\mathrm{v}_{x\_n} \;\; \mathrm{v}_{y\_n} \;\; \mathrm{v}_{z\_n}]^T$, the velocity vector, given in the coordinate system *n*

$\Psi = [\phi \;\; \theta \;\; \psi]^T$, the Euler angles vector

$\mathbf{C}_b^n =$ the rotation matrix from the body coordinate system *b* to the local coordinate system *n*

$\mathbf{E} =$ the Euler angles differential equations matrix

$\mathbf{a}^b = [a_{x\_b} \;\; a_{y\_b} \;\; a_{z\_b}]^T$, the acceleration vector, measured with respect to the body coordinate system *b*

$\boldsymbol{\omega}^b = [\omega_{x\_b} \;\; \omega_{y\_b} \;\; \omega_{z\_b}]^T$, the angular velocity vector (of the body axes) with respect to the inertial coordinate system.

The partial derivatives in eq. (10), the Jacobian matrix of the continuous, non-linear system of equations takes the form:

$$\mathbf{F} = \left.\frac{\partial \mathbf{f}(\mathbf{x}^*, \mathbf{u}_d)}{\partial \mathbf{x}}\right|_{\mathbf{x}=\mathbf{x}^*_{k-1}} = \begin{bmatrix} \mathbf{0} & \mathbf{I} & \mathbf{0} \\ \mathbf{0} & \mathbf{0} & (\mathbf{C}_b^n \cdot \mathbf{a}^b)'_{\boldsymbol{\Psi}} \\ \mathbf{0} & \mathbf{0} & (\mathbf{E} \cdot \boldsymbol{\omega}^b)'_{\boldsymbol{\Psi}} \end{bmatrix}_{\boldsymbol{\Psi}=\boldsymbol{\Psi}^*}, \tag{13}$$

with the explicit terms for our 2-D case (with the chosen set of state variables $\mathbf{x} = [s_x^n, s_y^n, \mathrm{v}_x^n, \mathrm{v}_y^n, \psi]^T$):

$$\left.\mathbf{C}_b^n\right|_{2-D} = \left.\mathbf{C}_b^n\right|_{f=0,q=0} = \begin{bmatrix} \cos\psi & -\sin\psi \\ \sin\psi & \cos\psi \end{bmatrix}, \tag{14}$$

$$\left.\mathbf{E}\right|_{2-D(\phi=0,\theta=0)} = [1]. \tag{15}$$

The 2-D form of the continuous, linearized system matrix (evaluated at the discrete time moments $t = t_k$, the beginning of the sampling intervals) becomes:

$$\left.\frac{\partial \mathbf{f}}{\partial \mathbf{x}}\right|_{\mathbf{x}=\hat{\mathbf{x}}_k^+} = \begin{bmatrix} 0 & 0 & 1 & 0 & 0 \\ 0 & 0 & 0 & 1 & 0 \\ 0 & 0 & 0 & 0 & -s\psi \cdot a_x^b - c\psi \cdot a_y^b \\ 0 & 0 & 0 & 0 & c\psi \cdot a_x^b - s\psi \cdot a_y^b \\ 0 & 0 & 0 & 0 & 0 \end{bmatrix}_{\mathbf{x}=\hat{\mathbf{x}}_k^+} \tag{16}$$

We obtain the approximate transition matrix $\boldsymbol{\Phi}_k = e^{\mathbf{F}\cdot\Delta t}$ [5], by assuming piecewise constancy of the deterministic inertial sensor signals during the sampling interval and by retaining only the linear term of the Taylor series:

$$\boldsymbol{\Phi}_k \cong \mathbf{I} + \mathbf{F} \cdot \Delta t \tag{17}$$

where Δt represents the small sampling rate interval.

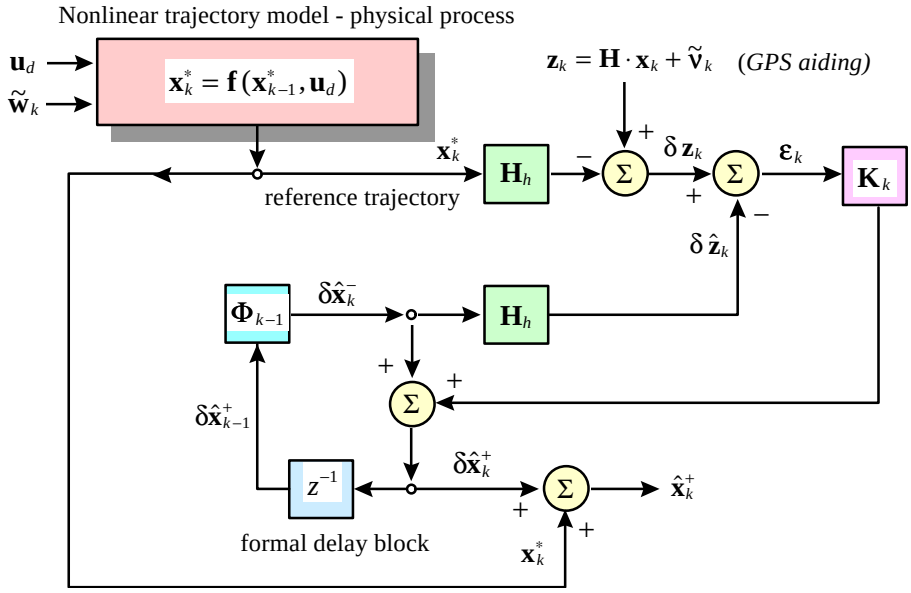

Fig. 11 *Discrete Linear Kalman Filter – a block diagram*

As we are observing here directly the states, the observation equation will be linear:

$$\mathbf{z}_k = \mathbf{H}_k \cdot \mathbf{x}_k + \tilde{\mathbf{v}}_k, \tag{18}$$

with the constant elements of the observation matrix $\mathbf{H}_k$. For the *CUPT* (Coordinate UPdaTe) the matrix $\mathbf{H}_k$ has only zero or unit elements (the positions are directly observed by *GPS*), as can be seen from the observation equations, written for the incremental state variables:

$$\begin{bmatrix} \delta\hat{z}^{-}_{s_x^n} \\ \delta\hat{z}^{-}_{s_y^n} \end{bmatrix}_k = \begin{bmatrix} 1 & 0 & 0 & 0 & 0 \\ 0 & 1 & 0 & 0 & 0 \end{bmatrix}_k \cdot \begin{bmatrix} \delta\hat{s}_x^{n-} \\ \delta\hat{s}_y^{n-} \\ \delta\hat{v}_x^{n-} \\ \delta\hat{v}_y^{n-} \\ \delta\hat{\psi}^{-} \end{bmatrix}_k . \qquad (19)$$

A block diagram for the Kalman filter operation is given in Fig. 11.

The formula set of the linearized approximation equations of the discrete recursive Kalman filter becomes [5]:

$$\delta\hat{\mathbf{x}}_k^- = \mathbf{\Phi}_{k-1} \cdot \delta\hat{\mathbf{x}}_{k-1}^+ \qquad (\textit{State Estimate Extrapolation})$$

$$\mathbf{P}_k^- = \mathbf{\Phi}_{k-1} \cdot \mathbf{P}_{k-1}^+ \cdot \mathbf{\Phi}_{k-1}^T + \mathbf{Q}_{k-1} \qquad (\textit{Covariance Estimate Extrapolation})$$

$$\mathbf{K}_k = \mathbf{P}_k^- \cdot \mathbf{H}_k^T (\mathbf{H}_k \cdot \mathbf{P}_k^- \cdot \mathbf{H}_k^T + \mathbf{R}_k)^{-1} \qquad (\textit{Filter Gain computation})$$

$$\delta\hat{\mathbf{x}}_k^+ = \delta\hat{\mathbf{x}}_k^- + \mathbf{K}_k \cdot (\mathbf{z}_k - \mathbf{H}_k \cdot \mathbf{x}_k^* - \mathbf{H}_k \cdot \delta\hat{\mathbf{x}}_k^-) \qquad (\textit{State Estimate Update})$$

$$\mathbf{P}_k^+ = (\mathbf{I} - \mathbf{K}_k \cdot \mathbf{H}_k) \cdot \mathbf{P}_k^- \qquad (\textit{Covariance Estimate Update})$$

The 2-D body-system components of the deterministic vector $\mathbf{u}_d = \left[\mathbf{a}^b \quad \boldsymbol{\omega}^b\right]^T$ - from the dynamic state equations (eq. 7, 12, 13, 16) - are computed using eq. (3) with the values of the components of the specific force vector $\mathbf{a}$ (a_x, a_y in [cm/s²]) and by direct scaling of the voltage signal output from the *z*-axis gyroscope (to obtain the angular rate ω_z^b [rad/s]). The conversion from the measured output voltages (*U* [V]) (of the *x/y* accelerometer channels and of the *z*-gyroscope channel), with the appropriate scaling, offset and non-orthogonality corrections, to $\mathbf{a}^b$ and $\boldsymbol{\omega}^b$ is:

$$\begin{bmatrix} a_x \\ a_y \end{bmatrix}_k = 1000 \cdot g_{IMAR} \cdot \begin{bmatrix} k\_acc\_xx & k\_acc\_yx \\ k\_acc\_xy & k\_acc\_yy \end{bmatrix} \cdot \begin{bmatrix} \frac{1}{skf\_acc\_x} & 0 \\ 0 & \frac{1}{skf\_acc\_y} \end{bmatrix} \cdot \begin{bmatrix} U\_acc\_x - U\_Offset\_acc\_x \\ U\_acc\_y - U\_Offset\_acc\_y \end{bmatrix}_k$$

and (20)

$$\omega_z^b\big|_k = \frac{\pi}{180} \cdot k\_gyro\_zz \cdot skf\_omega\_z \cdot (U\_omega\_z - U\_Offset\_omega\_z)_k . \qquad (21)$$

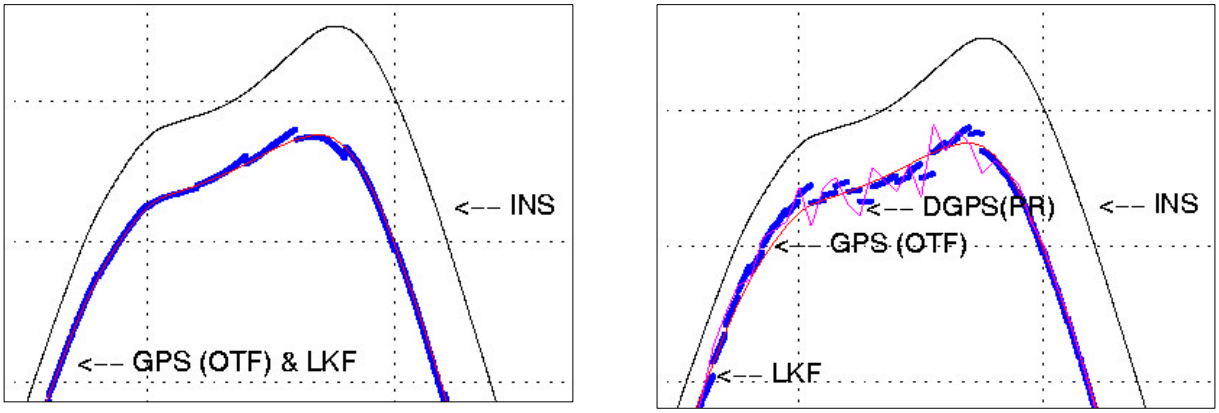

a. b.

Fig. 12 *Integrated solution for the x-component*
a - *carrier phase - DGPS solution, update every 4 s*
b - *pseudorange - DGPS solution, update every second*

As typical error standard deviations we considered for this application the following initial values, which enter into the error covariance matrices: for the system noise covariance matrix $\mathbf{Q}_k$ (assuming no correlation between the states) the initial values are assumed to be: $\mathbf{Q}_0 = diag(\sigma^2_{s\_x}, \sigma^2_{s\_y}, \sigma^2_{v\_x}, \sigma^2_{v\_y}, \sigma^2_{\psi\_z})$ with: $\sigma_{s\_x} = \sigma_{s\_y} = 5$ [m], $\sigma_{v\_x} = \sigma_{v\_y} = 2$ [m/s], $\sigma_{\psi\_z} = 0{,}01$ [rad]; for the observation error covariance matrix $\mathbf{R}_k$ we have taken a different set of values, differently weighing the model of the states/observation equation set of the Kalman filter. For the accuracy check of the integrated solution we have considered a diagonal matrix (without correlations between the observed states) with the structure: $\mathbf{R}_k = diag(\sigma^2_{s\_x}, \sigma^2_{s\_y}, \sigma^2_{v\_x}, \sigma^2_{v\_y}, \sigma^2_{\psi\_z})$, with elements: $\sigma_{s\_x} = \sigma_{s\_y} = .01$ [m], $\sigma_{v\_x} = \sigma_{v\_y} = 0.01$ [m/s], $\sigma_{\psi\_z} = 0{,}001$ [rad].

Although one could assume an infinite precision of the measurement for the initial phase of rest, we used finite values for the $\mathbf{R}_k$ terms, for algorithm stability reasons. The initial guess for the state covariance matrix $\mathbf{P}_0^-$ was the diagonal matrix $\mathbf{P}_0^- = diag(0{,}01;\ 0{,}01;\ 0{,}0001;\ 0{,}0001;\ 0{,}00001)$ - assuming also no correlation between the states**.** Performing in advance the alignment corrections, we have considered zero initial conditions for the dynamic system at rest: $\mathbf{x}_0^- = [0\ \ 0\ \ 0\ \ 0\ \ 0]^T$.

We used the van Loan algorithm [18] to update the system noise covariance matrix **Q**. To keep the symmetry of the positive-definite covariance matrix **P,** we enforced symmetry at each step of the algorithm. The prediction solution is computed with the speed of the sampling rate (0.04 s).

By using an *EKF* (Extended Kalman Filter) during the alignment phase, one can determine accurately the biases and the scale-factors of the inertial sensors (accelerometers and gyroscopes); after a short transient period, one obtains the values of those quantities.

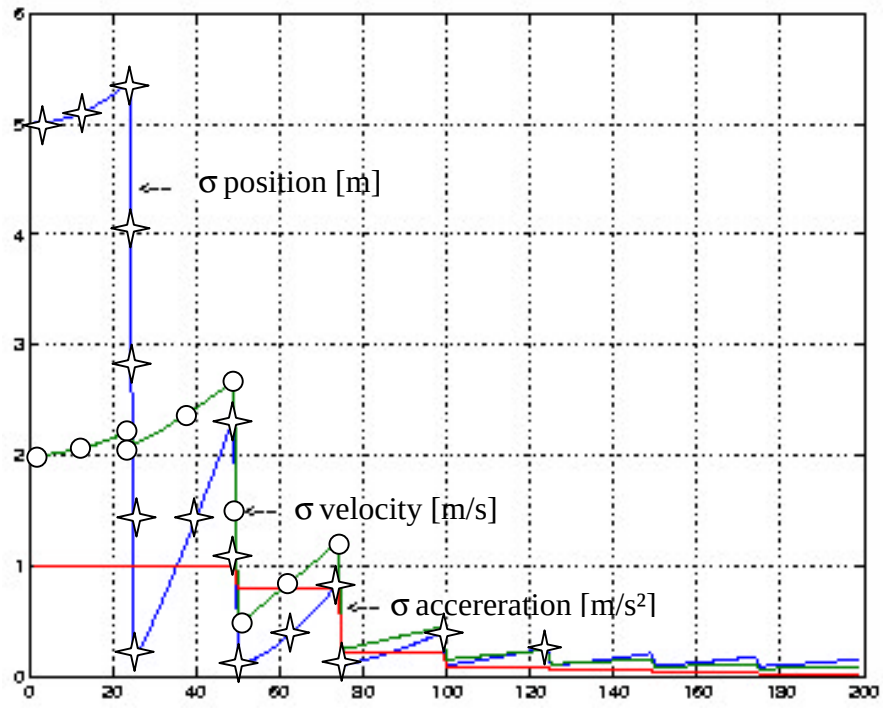

Fig. 13 *Evolution of the standard deviations for the LKF solution with DGPS aiding (updating every second)*
(x-axis divisions represent epochs of . 04 s)

Because of the relatively good fit of the 1 s aided *LKF* solution, we represent only the 4 s update solution (Fig. 12-a, for the *x* - component). In the figure are displayed the *IMU* strapdown solution - that is the reference trajectory for the *LKF* implementation -, the *carrier phase DGPS* high precision solution and the integrated global *KF* solution; one can see the characteristic aspect of the updating/estimation sequences. In Fig. 12-b a *LKF* solution is presented for the same *x* component with updates via a (simulated) *pseudorange DGPS* aiding.

Fig. 13 presents the evolution of the standard deviation (obtained as the square root of the appropriate diagonal terms of the covariance matrix **P**) of the principal state variables s, v for the filter process given in Fig. 12 - b.

The *x/y* Kalman filter solution of the strapdown *IMU* with regular *carrier phase DGPS* aiding is presented in Fig. 14, for both a 4 s update and a 1 s update.

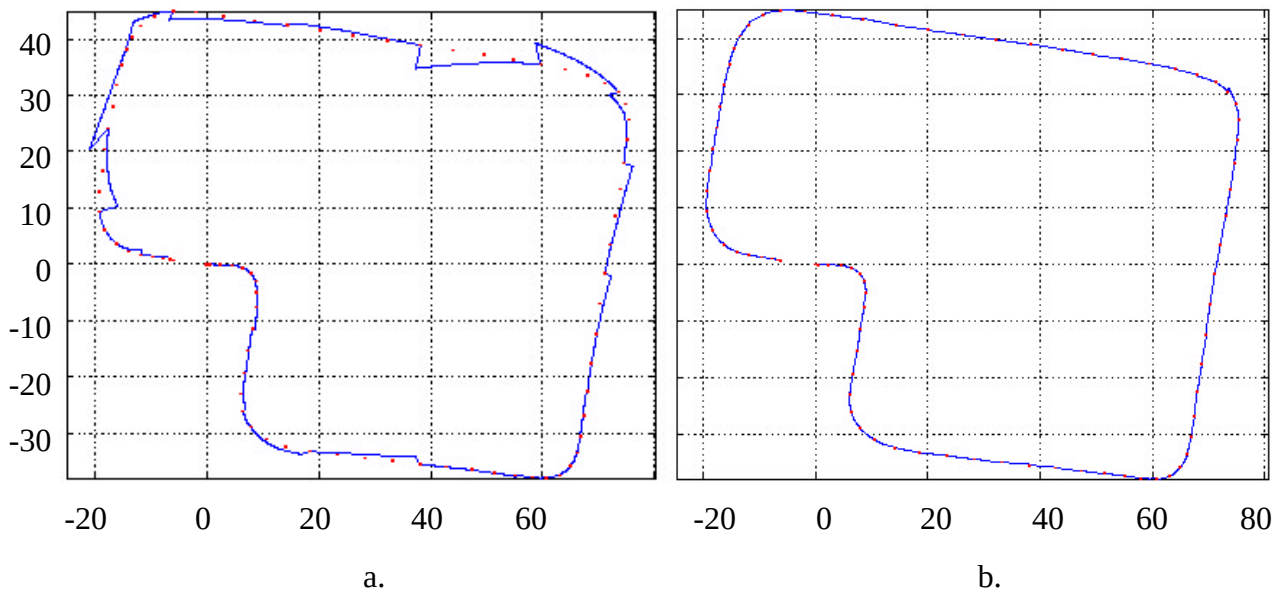

Fig. 14 *GPS - aided trajectories (LKF integrated solution) in [m]*
a – update every 4 s; b - update every 1 s

One can see that the 4 s solution is stronger perturbed than the 1 s solution and is no more acceptable; it allows for example hardly to discriminate between the two sides of the street.

VI. Conclusions

In the paper some preliminary results are presented from a *GPS*-aided *LKF* integrated trajectory solution for a low-cost strapdown mechanised *IMU*, using both precise carrier phase and pseudorange *DGPS* solutions. The precise *DGPS* reference trajectory enables the elaboration of a post-processing field evaluation methodology for the low-cost strapdown *IMU*. The obtained results encourage to more comprehensive investigations: drift modelling of the inertial sensors in the alignment procedure, calibration of the inertial sensors error sources and on-line navigation solutions with an *EKF* update are considered. Our hardware time-tagging solution enabled a precise absolute synchronisation of the two time-scales: of the *GPS* and of the *IMU*'s data acquisition. The integration *IMU/GPS* has permitted accuracies at the meter level for one second *DGPS* updating supported by the complementary nature of the error patterns of the *IMU* and of *GPS*. The precise carrier-phase *DGPS* solution (without signal-interruptions), with its accuracy at the *cm* level, provided a good reference for the performance evaluation of the strapdown mechanized *IMU*.
Because we were primarily interested to establish the integrated system feasibility, we have not modelled too extensively the actual inertial sensors. We intend to extend our analysis in order to achieve higher precision of the integrated solutions by the augmentation of the state variables set. Accelerometer biases, gyroscope drifts and inertial sensor scale-factor errors could be included - together with appropriate stochastic models - in order to better compensate for the systematic sensor errors. Furthermore, an increase of the inertial data acquisition rate would permit a better approximation of the non-linear dynamic model by a linear one. Finally, for a complete dynamic model one could consider the **g**-variations and the influence of the earth rotation, which enables the application of that analyse to more accurate *IMU*s, too.

Acknowledgment

Valuable suggestions by Prof. Dr. Reiner Rummel and fruitful discussions with Dr. Gerd Boedecker are gratefully acknowledged.

References

[1] - Knight, D., T. (1997): *"Rapid Development of Tightly-Coupled GPS/INS Systems"*, IEEE Transactions on Aerospace and Electronic Systems Magazine, Feb. 1997

[2] - Lemaire, Ch., Sulouff, B. (1995 - 1998): *"Surface Micromachined Sensors for Vehicle Navigation Systems"*, Analog Devices, Inc. (http://www.analog.com)

[3] - Doogen, M, Walsh, M (1997): *"The Design of a Track Map Based Data Acquisition System for the Darthmouth Formula Racing Team"*, Analog Devices, Inc. (http://www.analog.com)

[4] - Fa. iMAR (1995): "iMARtgac - *Installationshinweise, Korrekturmodell und Kalibrierung*" (Ggesellschaft für Mess-, Automatisierungs- und Regelsysteme)

[5] - Brown, R. G., Hwang, P. Y. C. (1997): "*Introduction to Random Signals and Applied Kalman Filtering*", 3-rd Edition, John Wiley & Sons Inc., New York

[6] - Grewal, M., S., Andrews, A., P. (1993): *"Kalman Filtering. Theory and practice"*, Prentice Hall, NJ

[7] - Böhm, M. (1997): *"Concepts for Hybrid Positioning"*, Symposium Gyro Technology 1997, Stuttgart, Germany

[8] - Krömer, O., Eggert, H., Fromhein, O., Gemmeke, H., Kühner, T., Lindermann, K., Mohr, J., Schulz, J., Strohrmann, M., Wollersheim, O. (1995): "*Intelligentes triaxiales Beschleunigungssensorsystem*", 2. Statuskolloquium des Projektes Mikrosystemtechnik im Forschungszentrum Karlsruhe, 28./29. November 1995

[9] - Baker, G. N. (1992): "*Quartz Rate Sensor from Innovation to Application*", Symposium Gyro Technology, Stuttgart 1992

[10] - Fa. National Instruments (1995): *"DAQPad -MIO-16XE-50, 16-Bit Data Acquisition and Control for the Parallel Port"*, User Manual, Austin

[11] - Time Service Department, U.S. Naval Observatory, Washington, DC (http://tycho.usno.navy.mil/frontpage.html)

[12] - Titterton, D., H., Weston, J., L. (1997): *"Strapdown inertial navigation technology"*, IEE Books, Peter Peregrinus Ltd., UK

[13] - Hofmann-Wellenhof, B., Lichtenegger, H., Collins, J. (1992): **"***GPS - Theory and Practice"*, Springer-Verlag, Wien

[14] - Leick, A. (1995): *"GPS Satellite Surveying"*, 2nd Edition, a Wiley-Interscience Publication, John Wiley & Sons, New York

[15] - Parkinson, B. W., Spilker J. J. Jr. (Editors) (1996): "*Global Positioning System: Theory and Applications*", Vol 163,-4: Progress in Astronautics and Aeronautics, Amer. Inst. Of Aeronautics and Astronautics, Inc., Washington

[16] - Blomenhofer, H. (1996): "*Untersuchungen zu hochpräzisen kinematischen DGPS-Echtzeitverfahren mit besonderer Berücksichtigung atmosphärischer Fehlereinflüsse*", Schriftenreihe Studiengang Vermessungswesen, Univerität der Bundeswehr München, Heft 51

[17] - Han, S., Rizos, C. (1997): "*Comparing GPS Ambiguity Resolution Techniques*", GPS World October 1997, pp. 54, Advanstar Communications, Cleveland

[18] - van Loan, C. F. (1978): „*Computing Integrals Involving the Matrix Exponential*", IEEE Trans. Automatic Control, AC - 23, 3 (June 1978)